Research Article

Short-term effects of the allelochemical umbelliferone on *Triticum durum* L. metabolism through GC-MS based untargeted metabolomics

Biswapriya B. Misra[1,], Vivek Das[2], Landi M.[3], Abenavoli M.R.[4], Araniti F.[4*]

[1]Center for Precision Medicine, Department of Internal Medicine, Section of Molecular Medicine, Wake Forest School of Medicine, Medical Center Boulevard, Winston-Salem 27157, NC USA.
[2]Novo Nordisk Research Center Seattle, Inc, Seattle, WA
[3]Department of Agriculture, Food and Environment, University of Pisa, Pisa, Italy
[4]Department AGRARIA, University Mediterranea of Reggio Calabria, – Località Feo di Vito, SNC I-89124 Reggio Calabria RC, Italy

*Corresponding author:
fabrizio.araniti@unirc.it
Department AGRARIA,
University Mediterranea of Reggio Calabria,
Località Feo di Vito,
SNC I-89124
Reggio Calabria RC,
Italy

Short title: *Wheat metabolomics of umbelliferone treatment*

Abstract

The present experiment used untargeted metabolomics to investigate the short-term metabolic changes induced in wheat seedlings by the specialized metabolite umbelliferone, an allelochemical. We used 10 day-old wheat seedlings treated with 104 µM umbelliferone over a time course experiment covering 6 time points (0 h, 6 h, 12 h, 24 h, 48 h, and 96 h), and compared the metabolomic changes to control (mock-treated) plants. Using gas chromatography mass spectrometry (GC-MS)-based metabolomics, we obtained quantitative data on 177 metabolites that were derivatized (either derivatized singly or multiple times) or not, representing 139 non-redundant (unique) metabolites. Of these 139 metabolites, 118 were associated with a unique Human Metabolome Database (HMDB) identifier, while 113 were associated with a Kyoto Encyclopedia of Genes and Genomes (KEGG) identifier. Relative quantification of these metabolites across the time-course of umbelliferone treatment revealed 22 compounds (sugars, fatty acids, secondary metabolites, organic acids, and amino acids) that changed significantly (repeated measures ANOVA, P-value < 0.05) over time. Using multivariate partial least squares discriminant analysis (PLS-DA), we showed the grouping of samples based on time-course across the control and umbelliferone-treated plants, whereas the metabolite-metabolite Pearson correlation revealed tightly formed clusters of umbelliferone-derived metabolites, fatty acids, amino acids, and carbohydrates. Also, the time-course umbelliferone treatment revealed that phospho-L-serine, maltose, and dehydroquinic acid were the top three metabolites showing highest importance in discrimination among the time-points. Overall, the biochemical changes converge towards a mechanistic explanation of the plant metabolic responses induced by umbelliferone. In particular, the perturbation of metabolites involved in tryptophan metabolism, as well as the imbalance of the shikimate pathways, which are strictly interconnected, were significantly altered by the treatment, suggesting a possible mechanism of action of this natural compound.

Keywords: metabolomics, gas chromatography mass-spectrometry, elicitation, polar, time-course, phytotoxicity, allelochemicals.

Introduction

Allelopathy is a complex ecological phenomenon, and refers to the direct and/or indirect effects of one organism (plant, insect, etc.) on another through the production and release of specialized

chemical compounds into the environment [1]. Due to the complexity of interpretation and analysis, the elucidation of allelopathy using chemical signatures is a challenge which requires expertise in diverse scientific fields, and the use of multidisciplinary tools and approaches [2]. In recent years, to unravel the ecological roles of specialized metabolites, rapid advancements have made use of *–omics* techniques and/or targeted and untargeted metabolic profiling of plant materials [3-6]. Techniques such as transcriptomics, proteomics, and metabolomics allow simultaneous analysis of the total molecular and biochemical constituents of a given sample [7]. In allelopathy studies, the use of metabolomics as an analytical technique allows identification and quantification of both primary and specialized metabolites in complex samples [8, 9]. Moreover, metabolomics is a useful tool in understanding the response to biotic and abiotic stress, for the determination of complex pathways of primary and specialized metabolite biosynthesis, and providing a broader understanding of biological activity and mode of action of critical specialized metabolites [6, 10]. In fact, metabolomics as a technique best represents the molecular phenotype, since it directly reflects the underlying biochemical activity and state of cells, tissues, and organism, being closest to the functional phenotype [11].

Among noteworthy allelochemicals, coumarins, which derive from the lactonization of o-hydroxycinnamic acid, is a class of specialized metabolites that are widely distributed in the plant kingdom, and they are synthesized by almost all higher plants [12], playing a pivotal role in both plant communication and defense [13]. One coumarin, umbelliferone, so named because of its wide occurrence within the Umbelliferae family, is an extremely biologically active compound widely distributed in the plant kingdom (Asteraceae, Rutaceae, Acanthaceae, and Hydrangeaceae, among others) [14]. Umbelliferone accumulates and is released to the environment through volatilization and root exudation [15-17]. The critical ecological role of umbelliferone has been demonstrated in several studies. For example, Minamikawa et al. [18] showed that umbelliferone production is induced in response to infection by plant pathogens. Similarly, it was noted, in the medicinal plant *Chamomilla recutita*, that under abiotic and biotic (powdery mildew *Erysiphe cichoracearum*) stress conditions, umbelliferone concentration increased to an extreme degree [19]. Those results suggest that this specialized metabolite could play a pivotal role in some plants as a first line of defense. This hypothesis was further confirmed by studies from Yang et al. [20], which highlighted its ability to suppress the *Ralstonia solanacearum*-induced wilting disease process by reducing fungi colonization and proliferation, and by Hamerski et al. [21], who demonstrated that extract of fungal cell wall acts as elicitor in *Amni majus*, increasing umbelliferone production. Umbelliferone is also involved in plant defense against herbivores, acting as a repellent interfering with the bitter gustatory receptor neurons of fruit flies [22]. Finally, it has been shown that umbelliferone determined the chemotactic

movement of *Rhizobium* and *Agrobacterium* across chemical gradients towards lower levels of inhibitors and higher levels of potential nutrients [23]. Concerning its phytotoxic potential, several studies have demonstrated that this molecule strongly affects both plant growth and development, inducing reactive oxygen species (ROS) accumulation, chlorophyll degradation, alteration of root morphology, and ROS-induced programmed cell death [24-26]. Moreland and Novitzy [27] found that umbelliferone, at relatively high concentrations, inhibits functions in isolated chloroplasts and mitochondria, whereas Einhellig [28] demonstrated that concentrations of umbelliferone that reduce *Glycine max* seedling growth also decreased leaf water potential, stomatal conductance, and the transpiration ratio.

Although several evidence regarding umbelliferone phytotoxicity are reported in the bibliography, such information is quite dated and does not unveil the metabolic pathways altered by the molecule. Moreover, it is widely known that allelochemicals could have a multi-target effect leading to a series of cascade effects, finally resulting in the inhibition of plant growth and/or plant death. Therefore, to identify their mode of action, it is important to focus attention on time-course experiments that evaluate the short term effects of these chemicals. This approach could lead to identifying the primary metabolic pathways affected. The main purpose of this study was to evaluate the short-term effect of umbelliferone on seedlings of durum wheat (*Triticum durum*) – a crop species often employed in phytotoxicity experiments due to its sensitivity to phytotoxins [29] – in order to identify the impact of this molecule on plant metabolism.

2. Materials and Methods

2.1. Chemicals and Reagents

Methanol for GC-MS SupraSolv® (1.00837), chloroform for GC-MS SupraSolv® (1.02432), N-Methyl-N-(trimethylsilyl) trifluoroacetamide (MSTFA) ≥98.5% (69479), pyridine ≥99% (270407), methoxyamine hydrochloride 98% (226904), umbelliferone 99% (H24003), ribitol ≥99% (A5502), and alkanes mixture C_{10}-C_{40} (68281) were acquired from Sigma Aldrich (Italy).

2.2 Plant growth conditions and elicitor treatments

Durum wheat (*Triticum durum* L. cv. Opera) seeds were germinated in Petri dishes (9 cm) in a growth chamber at 25°C, 70% humidity, with a photoperiod of 16 / 8 (light / dark), and light intensity of 90 mol m^{-2} s^{-1} supplied by a cool white fluorescent lamp (Polylux XL FT8, 55W 8440). Immediately

after germination, uniform seedlings were transferred to a 4.5 L hydroponic system and grown in a modified Hoagland solution formulated as follows: KNO_3 (10 mM); $MgSO_4$ (100 µM); $CaSO_4$ (400 µM); KCl (5 µM); K_2SO_4 (200 µM); K H_2PO_4 (175 µM); H_3BO_3 (2.5 µM); $MnSO_4$ (0.2 µM); $ZnSO_4$ (0.2 µM); $NaMoO_4$ (0.05 µM); $CuSO_4$ (0.05 µM); Fe-EDTA (200 µM). The solution was changed every other day and continuously oxygenated using an air bubble stone.

2.2.1 Dose-response curve

After the first true leaf formation (10 d from germination), wheat seedlings (a pool of 30 seedlings per replicate and treatment) were selected for uniformity in growth, and were transferred into continuously oxygenated hydroponic solutions enriched with different concentrations of umbelliferone: 0, 12.5, 25, 50, 100, 200, and 400 µM. After 10 days of treatment, the whole plants were collected, dried in an oven at 40°C, and weighed to monitor changes in total fresh weight (FW). Umbelliferone was first dissolved in ethanol (0.1%, w/v) and then poured into the nutrient solution prepared in deionized water. The same amount of ethanol was added to the mock treatments (control), and the experiment was replicated five times (n = 5).

2.2.2 Short-term effect of umbelliferone treatment

To study the short-term effects of umbelliferone on the wheat metabolome, seedlings (a pool of 10 seedlings per replicate, time point, and treatment) were grown for 10 days and were then treated with 104 µM of umbelliferone (the ED_{50} concentration was calculated from a dose-response curve). Plant materials were collected after 0 h (T0), 6 h (T1), 12 h (T2), 24 h (T3), 48 h (T4), and 96 h (T5) of umbelliferone treatment, and a parallel set of control plants (mock treated with same volume of ethanol as previously described) with the same time points. In order to avoid metabolic fluctuations induced by plant circadian rhythms, all the treatments were applied in order to allow plant collection at the same hour of the day (12:00) (i.e., plants belonging to treatment T1 were treated at 06:00, T2 at 00:00, and so on). After collection, the plant materials were immediately snap frozen for metabolomic studies. The experiment was replicated five times (n = 5).

2.3. Metabolite extraction and sample derivatization

Plant materials were collected at the middle of the light period, and whole plants were immediately snap frozen in liquid nitrogen to quench the endogenous metabolism. Freshly homogenized (100 mg) plant material was obtained from each biological sample (plant) and replicates. These were transferred to 2 mL microcentrifuge round bottom screw cap tubes (Eppendorf). Extraction was done by adding 1400 µL of methanol (at -20°C) and vortexing for 10 s after addition of 60 µL ribitol (0.2

mg/mL stock in ddH_2O) as an internal quantitative standard for the polar phase. Samples were transferred in a thermomixer at 70°C and were shaken for 10 min (950 rpm) and were then further centrifuged for 10 min at 11000 g. The supernatants were collected and transferred to glass vials where 750 µL $CHCl_3$ (-20°C) and 1500 µL ddH_2O (4°C) were sequentially added. All the samples were vortexed for 10 s and then centrifuged for another 15 min at 2200 g. Upper polar phase (150 µL) for each replicate was collected, transferred to a 1.5 mL tube and dried in a vacuum concentrator without heating. Before freezing and storing at -80°C, the tubes were filled with argon and placed in a plastic bag with silica beads (to avoid moisture and hydration during short-term storage). Before derivatization, stored samples were placed in a vacuum concentrator for 30 min to eliminate any trace of humidity. Then, 40 µL methoxyamine hydrochloride (20 mg/mL in pyridine) was added to the dried samples, which were then incubated for 2 h in a Thermomixer (950 rpm) at 37°C. Methoxyaminated samples were then silylated by adding 70 µL of MSTFA to the aliquots. Samples were further shaken for 30 min at 37°C. Derivatized samples (110 µL) were then transferred into glass vials suitable for the GC/MS autosampler for analysis.

2.4. GC-quadrupole/MS analysis

The derivatized extracts were injected into a TG-5MS capillary column (30 m x 0.25 mm x 0.25 µm) (Thermo Fisher Scientific, Waltham, MA, USA) using a gas chromatograph apparatus (Trace GC 1310, Thermo Fisher Scientific, Waltham, MA, USA) equipped with a single quadrupole mass spectrometer (ISQ LT, Thermo Fisher Scientific, Waltham, MA, USA). Injector and source were set at 250°C and 260°C, respectively. One µl of sample was injected in splitless mode with a helium flow of 1 mL/min using the following programmed temperature: isothermal 5 min at 70°C followed by a 5°C/ min ramp to 350°C and a final 5 min heating at 330°C. Mass spectra were recorded in electronic impact (EI) mode at 70 eV, scanning at 40-600 *m/z* range, scan time 0.2 s. Mass spectrometric solvent delay was settled as 9 min. Pooled samples that served as quality controls (QCs), n-alkane standards, and blank solvents (pyridine) were injected at scheduled intervals for instrumental performance, tentative identification, and monitoring of shifts in retention indices (RI).

2.5 GC/MS Analysis and data acquisition

2.5.1 GC/MS data analysis using MS-DIAL

Raw data (.RAW) from the single quadrupole instrument was converted to .mzML format with the MSConvertGUI from ProteoWizard. MS-DIAL, with open source publicly available EI spectra

194 library, was used for raw peaks extraction, and the data baseline filtering and calibration of the
195 baseline, peak alignment, deconvolution analysis, peak identification, and integration of the peak
196 height were essentially followed as described [30]. An average peak width of 20 scans and a minimum
197 peak height of 1000 amplitudes was applied for peak detection, and a sigma window value of 0.5, EI
198 spectra cut-off of 5000 amplitudes was implemented for deconvolution. For identification, the
199 retention time tolerance was 0.2 min, the *m/z* tolerance was 0.5 Da, the EI similarity cut-off was 60%,
200 and the identification score cut-off was 80%. In the alignment parameters setting process, the
201 retention time tolerance was 0.5 min, and retention time factor was 0.5. For MS-DIAL data
202 annotations, we used publicly available libraries (both positive and negative) for compound
203 identification, based on the mass spectral pattern as compared to EI spectral libraries such as NIST
204 Mass Spectral Reference Library (NIST14/2014; National Institute of Standards and Technology,
205 USA; with EI- MS data of 242,466 compounds), the MSRI spectral libraries from Golm Metabolome
206 Database [31] available from Max-Planck-Institute for Plant Physiology, Golm, Germany
207 (http://csbdb.mpimp-golm.mpg.de/csbdb/gmd/gmd.html), MassBank [32], and MoNA (Mass Bank
208 of North America, (http://mona.fiehnlab.ucdavis.edu/).For metabolite annotation and assignment of
209 the EI-MS spectra, we followed the metabolomics standards initiative (MSI) guidelines for metabolite
210 identification [33], i.e., Level 2: identification was based on spectral database (match factor >80%)
211 and Level 3: only compound groups were known, e.g. specific ions and RT regions of metabolites.
212
213 **2.6 Statistical analyses**
214 For metabolomic experiments, standard statistical analyses (summary statistics) were performed
215 using the statistical software R (Version 3.5.3, http://www.R-project.org) [34, 35]. Normalized
216 (internal standard), transformed (log2), imputed, and scaled peak areas representative of relative
217 metabolite amounts were obtained using DeviumWeb [36], and are presented in tables and figures.
218 Values reported in all tables and text are presented as means, and differences were considered
219 significant when $P < 0.05$ (nominal P-values).
220 The FW responses to different doses of umbelliferone were evaluated by a nonlinear regression model
221 using a log-logistic equation, largely employed in phytotoxicity screenings [37] that allowed to
222 estimate the ED50 parameter, the dose required to reduce 50% of the total response. The ED_{50} value
223 was then used as the key concentration for the short-term metabolomics experiments.
224
225 **2.6.1 Univariate analysis**
226 ANalysis Of VAriance (ANOVA) was performed using R. Hierarchical clustering analysis (HCA)
227 using average linkage clustering was performed on Pearson distances from the metabolite abundance

data, using PermutMatrix [38]. For heat maps, data were normalized using the z-scores of the intensity counts for each of the metabolites under the peak areas.

2.6.2 Multivariate analysis

Exploratory multivariate analysis was done using R (version 3.6.1). The sample-sample distance clustering was obtained via package Pheatmap, using Pearson correlation and default parameters. The exploratory interactive MDS plots were done with the Glimma package. Other various dimension reduction analysis via principal component analysis (PCA) of overall, separate control, and treated data was performed with the FactoMineR and factoextra packages. PCA and partial least-squares discriminant (PLS-DA) analyses were performed using the DeviumWeb package [39], where the output consisted of score plots to visualize the contrast between different samples and loading plots to explain the cluster separation. Data were scaled with unit variance, without any transformation. Partial least-squares discriminant analysis (PLS-DA) was used to highlight differences between the metabolic phenotypes at six time points (0 h, 6 h, 12 h, 24 h, 48 h, and 96 h).

2.7 Time-course analysis of control and umbelliferone-treated metabolomes

For short time series metabolomics data analysis, we used the Short Time series Expression Miner (STEM) tool [40], originally used for short microarray time series experiments (3–8 time points for >~80% of the datasets). The novel STEM clustering takes advantage of the few time points in a dataset, and it first selects a set of distinct and representative temporal expression profiles (i.e., model profiles), where these model profiles are independent of data. The clustering algorithm then assigns each feature (i.e., metabolite) passing the filtering criteria to the model profile that most closely matches the feature's abundance profile as determined by the correlation coefficient, and determines which profiles have a statistically significant higher number of features assigned using a permutation test. STEM was used as a Java implementation with a graphical user interface, available at http://www.cs.cmu.edu/~jernst/st/ for clustering the metabolite accumulation patterns according to time points. For our analysis, we used the following criteria: no additional normalization of the data; 0 added as the starting point; number of model profiles = 20; maximum unit change in model profiles between time points = 3. To explain the model profiles, we used an expression of -1 for decreased levels of a metabolite, 0 for unchanged levels of a metabolite, and 1 for increased levels of a metabolite. For instance, a model profile with an expression of -1, -1, 0, 1, 1, 0 represents decreased, decreased, unchanged, increased, increased, and unchanged levels of a given set of metabolites for the 6 time points in the given model profile.

2.8 Pathway enrichment and clustering analysis

Pathway enrichment analysis was performed at MetaboAnalyst (www.Metaboanalyst.ca) [41], and Chemical Translation Service (CTS: http://cts.fiehnlab.ucdavis.edu/conversion/batch) was used to convert the common chemical names into their Kyoto Encyclopedia of Genes and Genomes (KEGG), Human Metabolome Database (HMDB), CAS, PubChem Compound ID (CID), LipidMAPS IDs and InChiKeys identifiers.

2.9 Data sharing

The raw datasets and the metadata obtained from the GC-EI-MS platform have been deposited at the Metabolomics Workbench (Study ID: **ST001056**, http://dx.doi.org/10.21228/M81M4X).

3. Results and Discussion

3.1 Dose response curve based on wheat biomass production in response to umbelliferone

The dose response curve built on the variation of wheat fresh biomass (FW), in response to increasing doses of umbelliferone (0-400 µM), pointed out a significant dose-dependent phytotoxic effect (**Fig. 1**). The lowest concentration (12.5 µM) did not affect plant growth. At 25 µM, a 17% reduction of biomass was observed, and the reduction reached 82% at the highest concentration (400 µM). The non-linear regression fit of FW raw data determined an ED_{50} value of 104 µM. Inhibitory effects of umbelliferone to plants such as *Festuca rubra*, *Medicago sativa* and *Lactuca sativa* have been reported [17, 42]. Based on the optimized umbelliferone concentration, we designed the experiment to investigate the metabolomic changes in seedlings exposed to 6 h, 12 h, 24 h, 48 h, and 96 h of umbelliferone treatment, as compared with the controls (mock treated) (**Figure 2**).

3.2 **Cataloging the wheat seedling metabolome**

Using GC-MS, we obtained quantitative data on 177 metabolites that were derivatized (either derivatized singly or multiple times) or not, representing 139 non-redundant (unique) metabolites. Of these 139 metabolites, 118 were associated with a unique HMDB identifier, while 113 were associated with a KEGG identifier. The derivatized metabolites included sugars (monosaccharides,

disaccharides), sugar alcohols, sugar acids, dipeptides, organic acids, amino acids, phosphates, polyamines, purines, and pyrimidines, while the non-derivatized metabolites included fatty acids, among others. We also captured several known secondary / specialized metabolites such as phenolic compounds (polyphenols and flavonoids), i.e., pyrocatechol, protocatechuic acid, chlorogenic acid, pyrogallol, homovanillate, sinapaldehyde, catechin, caffeine, and myricetin; and others, such as phytol and quinolinic acid. We also captured the modified (metabolized) forms of umbelliferone, i.e., 4-methylumbelliferone and psoralen. These metabolites belonged to 50 different KEGG-based metabolic pathways (**Supplementary Figure 1)**, with the top pathways belonging to arginine and proline metabolism, glutathione metabolism, aminoacyl-tRNA biosynthesis (all P-value < 0.05), taurine and hypotaurine metabolism, tryptophan metabolism, beta-alanine metabolism, isoquinoline alkaloid biosynthesis, phenylalanine, tyrosine and tryptophan metabolism, alanine, aspartate and glutamate metabolism (all P-value < 0.1), and indole alkaloid biosynthesis, among others **(Supplementary Figure 2)**.

3.3 Impact of umbelliferone on wheat metabolome

Umbelliferone is an extremely biologically active coumarin widespread in the Umbelliferae family, but also in other genera, in plant families such as Asteraceae, Rutaceae, Acanthaceae, and Hydrangeaceae [14]. A huge body of research has clearly demonstrated that application of umbelliferone can lead to phytotoxic effects, thereby affecting both plant growth and development [24, 26-28]. We performed a one-way ANOVA on each compound, to test if at least one level of time had a mean average significantly different form the rest. There are 22 significant compounds (sugars, fatty acids, secondary metabolites, organic acids, and amino acids) with p-value lower than 0.05 (**Table 1**). To control for false positive findings, a False Discovery Rate (FDR) was applied to the nominal p-values; 7 compounds (sugars: maltose, xylulose, ribose, 6-deoxyglucose) were still significant after the FDR correction.

3.4 Time-course profiling of umbelliferone treatment (quantitative)

To understand the time-course-dependent changes in metabolite accumulation patterns across the treatment groups in this complex study design, we started with a clustering analysis. Using short time-series expression miner (STEM) analysis, we interrogated the time-course changes of the metabolites

for further analysis. The metabolite abundances for 177 metabolites across the 6 time points were put into 20 model clusters, which revealed differential accumulation of metabolites for control and umbelliferone-treated groups of plants, as a function of time. In the case of the control plants, the most significant model cluster (number 10, with 18 metabolites, P-val, 2E-3) showed a 0, 1, 0, 1, -1, 1 pattern (where 0 is no change, 1 is increase, and -1 is decrease) for the six time-points in the study [0 h (T0), 6 h (T1), 12 h (T2), 24 h (T3), 48 h (T4), and 96 h (T5)]. These 18 metabolites were sugars (fucose, maltose, trehalose, and xylulose), organic acids (isohexonic acid, tranexamic acid, and aconitic acid), amines (pyridoxamine, tryptamine), ribulose 1, 5-bisphosphate, 3-indoleacetonitrole, etc. (**Figure 3 A, B**). In the case of umbelliferone-treated plants, the most significant model cluster (number 9, with 13 metabolites, P-val, 4E-4) showed a 0, 1, -1, -1, 1, -1 pattern for the six time-points in the study. These 13 metabolites were sugars (trehalose, xylulose, melibiose, and rhamnose), organic acids (ascorbic acid, pimelic acid, quinolic acid, and aconitic acid) polyamines (putrescine and spermidine), etc. (**Figure 3 C, D**).

3.5 Multivariate and clustering analysis reveal metabolites

Secondly, we performed both supervised and unsupervised multivariate analyses as feature extraction strategies, to maximize variance in the data using strongly correlated variables. We first performed an unsupervised analysis, which explained ~40–43% of the variability in data using the first 2 PCs, either in all samples grouped together, only control sample groups, or umbelliferone groups (**Supplementary Figure 8A-C)**. However, the time points did not cluster well, which points to the non-independent samples which are not well handled by PCA, the small feature space of 177 metabolites, and too many treatments (6 time points x 2 treatments), leading to possible multicollinearity issues, displaying more artifacts than a true biological picture. Following the lack of clustering in the PCA, we performed PLS-DA separately for both control and umbelliferone treatment groups, where time-point based groupings were observed. Using supervised PLS-DA analysis for all the samples (all time points, control and umbelliferone treated plants) and the blanks (B), we showed that the first two components explained variations from the T0, 6 h, 12 h, 24 h, 48 h, and 96 h time points; components 1 and 2 alone explained ~45% of the variation (**Figure 4A**). For the control and umbelliferone-treated plants, the first two components (1 and 2) helped explain ~14% and ~15% of the variations, respectively (**Figures 4B, C**). The co-clustering of time points (i.e., 6 h with 96 h) could point to interesting biological phenomena, such as the appearance of two peaks, one in very short-term defense response and another sustained one later. These are speculations, and

would be very difficult to validate further using metabolomics experiments and the premises of this study.

Using metabolite-metabolite (Pearson) correlation, we monitored the clusters of metabolites. Among secondary metabolites, we found that 3-indoleacetonitrile (an auxin, from tryptophan metabolism), psoralen and 4-methylumbelliferone (both umbelliferone derivatives), and 2-coumaric acid were highly correlated (**Supplementary Figure 3, 4)**, indicating their possibly coordinated biosynthesis and regulation. Similarly, tight clusters were observed for fatty acids (**Supplementary Figure 5**), groups of amino acids (**Supplementary Figure 6**), and carbohydrates (**Supplementary Figure 7)**. A recent study that looked at various polyphenols across diverse species observed that umbelliferone and kaempferol are quantitatively associated with each other, while there was a positive correlation of epicatechin with umbelliferone and kaempferol [43].

In order to identify the metabolites responsible for the discrimination among the metabolomic profiles, the VIP scores were used to select those with the most significant contributions in a PLS-DA model, thus as a measure of a variable's importance in the PLS-DA model. VIP scores are a weighted sum of PLS weights for each variable, and measure the contribution of each predictor variable to the model [44]. The VIP statistic indicates the importance of the metabolites in differentiating the study groups (umbelliferone treatment times, i.e., 0 h, 6 h, 12 h, 24 h, 48 h, 96 h) in multivariate space. The compounds exhibiting the higher VIP scores are the more influential variables. Our VIP analysis revealed that the metabolites with high VIPs were phospho-L-serine, maltose, dehydroquinic acid, pyrocatechol, tryptamine, and serotonin, among others **(Figure 5)**. Thus, the biochemical changes induced by umbelliferone treatment may support mechanistic explanations of the plant metabolic responses induced by this coumarin compound. In particular, as highlighted by the VIP scores reported (**Figure 5**), several metabolites involved in both shikimate and tryptophan pathways were significantly altered by the treatment. Among them, fluctuations in dehydroquinic acid abundances during all the treatments are noteworthy, where the highest values were recorded at 12 h and 96 h. Dehydroquinic acid represents the first carbocyclic intermediate of the shikimate pathway, which undergoes five further enzymatic steps in the remainder of the shikimate pathway to yield chorismic acid, a precursor to tyrosine, phenylalanine, tryptophan, and some vitamins [45]. Interestingly, pyridoxamine (vitamin B6) was significantly altered by the umbelliferone treatment; it reached highest abundance at 24 h of treatment, dropped after 48 h, and increased again at 96 h; it is an essential coenzyme with a high antioxidant potential [46]. Moreover, pyridoxamine in the presence of ATP is converted by the pyridoxal kinase in pyridoxal 5'-phosphate,

which is strictly connected to the enzyme tryptophan synthetase, an enzyme that catalyses the final two steps in the biosynthesis of tryptophan [47]. The tryptophan synthetase, typically found as a α2β2 tetramer, catalyses the irreversible condensation of indole and serine to form tryptophan in a pyridoxal 5'-phosphate-dependent reaction [48]. In addition, the conversion of tryptophan to indole acetic acid leads to the formation of glutamate, which is one of the pyridoxamine precursors [49]. It is therefore conceivable that, as detailed below, the umbelliferone-triggered perturbation of the tryptophan metabolism might be on the basis of the observed pyridoxamine accumulation pattern over time. It is also possible that the fluctuation in pyridoxamine content is attributable to the conversion into their derivatives, namely pyridoxal, pyridoxal 5-phosphate, and pyridoxamine [50], involved in many other cellular functions, which were simply not detected / quantified in our metabolomics experiments. Among the metabolites involved in tryptophan biosynthesis, phospho-L-serine [51] was characterized by the highest VIP score, pointing to a significant increase in concentration over time. This molecule has a pivotal role in plants under environmental stresses, as an upregulation of several genes involved in this pathway were observed during abiotic stresses such as salinity, cold, and flood, indicating its importance in supplying serine under environmental stresses [52]. Moreover, the phosphorylated pathway might be essential to provide the amino acid serine for the synthesis of tryptophan, the common precursor for the biosynthesis of indole acetic acid (IAA) [53]. Interestingly, in our experiments, significant variations in IAA and tryptamine (indole-alkaloid) content, an intermediate in IAA biosynthesis, were observed. In fact, both metabolites were significantly elicited by the umbelliferone treatment. Alteration in IAA biosynthesis and distribution, driven by 4-methylumbelliferone (an umbelliferone derivative), was previously observed by Li et al. [25] in *Arabidopsis* seedlings. In particular, they observed that the exogenous application of 4-methylumbelliferone (125 μM for 22 days) led to reduced primary root growth, the formation of bulbous root hairs, and an increase in the number of lateral roots. The authors also uncovered an accumulation of 4-methylumbelliferyl-β-D-glucoside, derived from UDP-glycosyltransferase mediated transformation of umbelliferone in roots and upregulation of several *UDP-glycosyltransferase* genes, which were supportive for a well-orchestrated mechanism devoted to the detoxification of umbelliferone in plants. During our experiments, the presence of both 4-methylumbelliferone and psoralen, umbelliferone derivatives, was detected in umbelliferone-treated plants, suggesting that the umbelliferone was internalized and metabolized by the seedlings.

Studies of several other species have proven that both umbelliferone derivatives can act as phytoalexins themselves; they can protect plants from both biotic and abiotic stresses, and/or can induce reduction in growth and development [25, 54-56]. Therefore, it cannot be excluded that the reduction in plant growth observed during the dose response curve could also be due to the

accumulation of umbelliferone derivatives. Recent studies of *Psoralea corylifolia*, treated with psoralen elicitors and precursors, demonstrated that there is a negative correlation between psoralen accumulation and cell growth [57]. Furthermore, psoralen accumulation in plants, as well as other specialized metabolites, play a pivotal role in protecting plants from several other stresses [57], and the observed plant growth reduction is probably due to the redistribution of plant energies in the activation of (specialized) biosynthetic pathways involved in detoxification and/or protection from oxidative stress, instead of the biosynthesis of (primary) metabolites fundamental for growth.

Despite its role as an intermediate in auxin biosynthesis, it has been suggested that tryptamine could play an important role during both biotic and abiotic stress. It has been observed, for example, that barley leaves irradiated with UV light were accumulating high levels of tryptamine. Moreover, its induction was also observed to occur in response to plant pathogenic fungi infection, suggesting that it could act as a plant defense metabolite [58]. On the other hand, tryptamine accumulation was accompanied by a reduction in serotonin content. It has been widely reported that in graminaceous species the enzyme tryptamine 5-hydroxylase is involved in serotonin biosynthesis, catalyzing the conversion of tryptamine to serotonin [59, 60]. Kang et al. [61] demonstrated that the exogenous application of tryptamine to tissues of rice seedlings induced a dose-dependent increase in serotonin, accompanied by a parallel increase in tryptamine 5-hydroxylase enzyme activity. At the same time, the same tissues grown in the presence of tryptophan did not show any significant increase in serotonin. Therefore, it can be speculated that tryptamine accumulation, followed by the reduction in serotonin content, could be due to an umbelliferone-induced reduction of tryptamine 5-hydroxylase activity. Serotonin, which plays a pivotal role in plant growth regulation and in plant response to both biotic and abiotic stress [62], and psoralen, are considered to be phytoalexins with antioxidant properties involved in plant defense [55].

Limitations of the study

Our study has several limitations. First, separating sample preparations based on separate analysis of shoots and roots, or leaf analysis, would have provided more spatial information on organ- and plant part-specific metabolic changes, which may have confounded the analysis in this whole seedling analysis approach. Secondly, the overall feature space (i.e., the number of metabolites) is also very limited. Our current total metabolites quantified ($p = 177$) is roughly three times the overall sample size ($n = 53$). Hence, the data is limited in dimensionality. These metabolites are also highly correlated both at intra- and inter-group levels, limiting the overall variance contributions. High correlations can also contribute to multicollinearity. All of these factors, taken together, limit the overall results and

interpretations of the current study. Lastly, techniques other than mass-spectrometry-based analysis, i.e., additional orthogonal technique such as liquid chromatography-mass-spectrometry (LC-MS) with wider metabolic coverage and less complex sample preparations steps (i.e., drying and derivatization), may have been helpful in the identification and relative quantification of various metabolites belonging to more numbers of pathways, and capturing multiple secondary metabolites involved in plant stress metabolic responses.

4. Conclusions

This study clearly shows the system-wide metabolomic changes in wheat seedlings in response to umbelliferone treatment. Although this molecule has been studied extensively, this is the first time a short-term experiment using sub-lethal concentrations has been carried out. This untargeted metabolomics approach allowed us to identify the system-wide metabolic responses activated by the plants to deal with this phytotoxic compound. Among them, one of the first responses activated by plants was the internalization of umbelliferone into its derivative psoralen. In addition, umbelliferone induced a system-wide change through the dysregulation of metabolites involved in the shikimate pathways, as well as in tryptophan and tryptamine metabolism. This study provides new insights into the early response of plants to this specialized metabolite. Thus, taken together our work can be used as a reference for further studies aimed at clarifying its mode of action.

Acknowledgments

This research was supported by the Italian Ministry of Education, University and Research (MIUR), project SIR-2014 cod. RBSI14L9CE (MEDANAT).

Author Contributions

FA, BBM and MRA conceived and designed the study; FA and ML performed the experiments; BBM, VD, FA analyzed the data; FA and MRA contributed reagents/materials/analysis tools; BBM, FA, MRA and ML wrote the paper.

Conflicts of Interest

VD currently works as a Post-Doctoral Researcher in Novo Nordisk Research Center Seattle, Inc; however, he did not receive any funding for this work. All authors declare that they had no conflicts of interest.

5. References

[1] S. Rizvi, H. Haque, V. Singh, V. Rizvi, A discipline called allelopathy, in: Allelopathy, Springer, 1992, pp. 1-10.

[2] F. Araniti, M. Scognamiglio, A. Chambery, R. Russo, A. Esposito, B. D'Abrosca, A. Fiorentino, A. Lupini, F. Sunseri, M.R. Abenavoli, Highlighting the effects of coumarin on adult plants of *Arabidopsis thaliana* (L.) Heynh. by an integrated-omic approach, J. Plant Physiol. 213 (2017) 30-41.

[3] B. D'Abrosca, M. Scognamiglio, V. Fiumano, A. Esposito, Y.H. Choi, R. Verpoorte, A. Fiorentino, Plant bioassay to assess the effects of allelochemicals on the metabolome of the target species *Aegilops geniculata* by an NMR-based approach, Phytochem. 93 (2013) 27-40.

[4] M. Scognamiglio, B. D'Abrosca, A. Esposito, A. Fiorentino, Metabolomics: an unexplored tool for allelopathy studies, J. Allelochem. Int. 1 (2015) 9-21.

[5] F. Araniti, A. Lupini, F. Sunseri, M.R. Abenavoli, Allelopatic potential of *Dittrichia viscosa* (L.) W. Greuter mediated by VOCs: a physiological and metabolomic approach, PloS one, 12 (2017) e0170161.

[6] F. Araniti, A. Lupini, A. Mauceri, A. Zumbo, F. Sunseri, M.R. Abenavoli, The allelochemical trans-cinnamic acid stimulates salicylic acid production and galactose pathway in maize leaves: A potential mechanism of stress tolerance, Plant Physiol. Biochem. 128 (2018) 32-40.

[7] S.O. Duke, J. Bajsa, Z. Pan, Omics methods for probing the mode of action of natural and synthetic phytotoxins, J. Chem. Ecol. 39 (2013) 333-347.

[8] J. Lisec, N. Schauer, J. Kopka, L. Willmitzer, A.R. Fernie, Gas chromatography mass spectrometry–based metabolite profiling in plants, Nat. Protoc. 1 (2006) 387.

[9] F. Araniti, T. Gullì, M. Marrelli, G. Statti, A. Gelsomino, M.R. Abenavoli, *Artemisia arborescens* L. leaf litter: phytotoxic activity and phytochemical characterization, Acta Physiol. Plant. 38 (2016) 128.

[10] U. Roessner, A. Luedemann, D. Brust, O. Fiehn, T. Linke, L. Willmitzer, A.R. Fernie, Metabolic profiling allows comprehensive phenotyping of genetically or environmentally modified plant systems, The Plant Cell. 13 (2001) 11-29.

[11] O. Fiehn, Metabolomics—the link between genotypes and phenotypes, in: Functional genomics, Springer, 2002, pp. 155-171.

[12] S. Brown, A. Zobel, Biosynthesis and distribution of coumarins in the plant, in: Proceedings of the Conference «Coumarins: Research and Applications», Padua, Italy, 1990, pp. 20-22.

[13] A. Zobel, S. Brown, Coumarins in the interactions between the plant and its environment, Allelopathy J. 2 (1995) 9-20.

[14] O. Mazimba, Umbelliferone: sources, chemistry and bioactivities review, Bulletin of Faculty of Pharmacy, Cairo University, 55 (2017) 223-232.

[15] E. Haggag, I. Mahmoud, E. Abou-Moustafa, T. Mabry, Coumarins, fatty acids, volatile and non-volatile terpenoids from the leaves of *Citrus aurantium* L.(sour orange) and *Citrus sinensis* (L.) Osbeck (sweet orange), Asian J. Chem. 11 (1999) 784-789.

[16] S. Yaoya, H. Kanho, Y. Mikami, T. Itani, K. Umehara, M. Kuroyanagi, Umbelliferone released from hairy root cultures of Pharbitis nil treated with copper sulfate and its subsequent glucosylation, Biosci. Biotech. Biochem. 68 (2004) 1837-1841.

[17] H. Guo, H. Cui, H. Jin, Z. Yan, L. Ding, B. Qin, Potential allelochemicals in root zone soils of *Stellera chamaejasme* L. and variations at different geographical growing sites, Plant Growth Regul. 77 (2015) 335-342.

[18] T. Minamikawa, T. Akazawa, I. Uritani, Analytical study of umbelliferone and scopoletin synthesis in sweet potato roots infected by *Ceratocystis fimbriata*, Plant Physiol. 38 (1963) 493.

[19] M. Repčák, J. Imrich, M. Franeková, Umbelliferone, a stress metabolite of *Chamomilla recutita* (L.) Rauschert, J. Plant Physiol. 158 (2001) 1085-1087.

[20] L. Yang, S. Li, X. Qin, G. Jiang, J. Chen, B. Li, X. Yao, P. Liang, Y. Zhang, W. Ding, Exposure to umbelliferone reduces *Ralstonia solanacearum* biofilm formation, transcription of type III secretion system regulators and effectors and virulence on tobacco, Front. Microbiol. 8 (2017) 1234.

[21] D. Hamerski, R.C. Beier, R.E. Kneusel, U. Matern, K. Himmelspacht, Accumulation of coumarins in elicitor-treated cell suspension cultures of *Ammi majus*, Phytochem. 29 (1990) 1137-1142.

[22] L.A. Weiss, A. Dahanukar, J.Y. Kwon, D. Banerjee, J.R. Carlson, The molecular and cellular basis of bitter taste in Drosophila, Neuron. 69 (2011) 258-272.

[23] A. Brencic, S.C. Winans, Detection of and response to signals involved in host-microbe interactions by plant-associated bacteria, Microbiol. Mol. Biol. Rev. 69 (2005) 155-194.

[24] E. Kupidlowska, M. Kowalec, G. Sulkowski, A. Zobel, The effect of coumarins on root elongation and ultrastructure of meristematic cell protoplast, Ann. Bot. 73 (1994) 525-530.

[25] X. Li, M.Y. Gruber, D.D. Hegedus, D.J. Lydiate, M.-J. Gao, Effects of a coumarin derivative, 4-methylumbelliferone, on seed germination and seedling establishment in Arabidopsis, J. Chem. Ecol. 37 (2011) 880.

[26] L. Pan, X.-z. Li, Z.-q. Yan, H.-r. Guo, B. Qin, Phytotoxicity of umbelliferone and its analogs: Structure–activity relationships and action mechanisms, Plant Physiol. Biochem. 97 (2015) 272-277.

[27] D.E. Moreland, W.P. Novitzky, Effects of phenolic acids, coumarins, and flavonoids on isolated chloroplasts and mitochondria, Allelochemicals: role in agriculture and forestry, 330 (1987) 247-261.

[28] F. Einhellig, The physiology of allelochemical action: clues and views, Allelopathy from molecules to ecosystems, (2002) 1-23.

[29] F.A. Macías, D. Castellano, J.M. Molinillo, Search for a standard phytotoxic bioassay for allelochemicals. Selection of standard target species, J. Agricul. Food Chem. 48 (2000) 2512-2521.

[30] H. Tsugawa, T. Cajka, T. Kind, Y. Ma, B. Higgins, K. Ikeda, M. Kanazawa, J. VanderGheynst, O. Fiehn, M. Arita, MS-DIAL: data-independent MS/MS deconvolution for comprehensive metabolome analysis, Nat. Meth. 12 (2015) 523.

[31] J. Kopka, N. Schauer, S. Krueger, C. Birkemeyer, B. Usadel, E. Bergmüller, P. Dörmann, W. Weckwerth, Y. Gibon, M. Stitt, GMD@ CSB. DB: the Golm metabolome database, Bioinformatics, 21 (2004) 1635-1638.

[32] H. Horai, M. Arita, S. Kanaya, Y. Nihei, T. Ikeda, K. Suwa, Y. Ojima, K. Tanaka, S. Tanaka, K. Aoshima, MassBank: a public repository for sharing mass spectral data for life sciences, J. Mass Spectr. 45 (2010) 703-714.

[33] S.-A. Sansone, T. Fan, R. Goodacre, J.L. Griffin, N.W. Hardy, R. Kaddurah-Daouk, B.S. Kristal, J. Lindon, P. Mendes, N. Morrison, The metabolomics standards initiative, Nat. Biotech. 25 (2007) 846.

571 [34] R.C. Team, R: A language and environment for statistical computing; 2015, in, 2018.

572 [35] F.J. Rohlf, R.R. Sokal, Statistical tables, Macmillan, 1995.

573 [36] D. Grapov, DeviumWeb: version 0.3.2. ZENODO doi:10.5281/zenodo.12879,
574 https://github.com/dgrapov/DeviumWeb, (2014).

575 [37] R.G. Belz, K. Hurle, S.O. Duke, Dose-response—a challenge for allelopathy?, Nonlin. Biol.
576 Toxic. Med. 3 (2005) nonlin. 003.

577 [38] G. Caraux, S. Pinloche, PermutMatrix: a graphical environment to arrange gene expression
578 profiles in optimal linear order, Bioinformatics 21(7) (2005) 1280-1281 (2014).

579 [39] D. Grapov, DeviumWeb: Version 0.3.2. ZENODO. https://doi. org/10.5281/zenodo.12879,
580 https://github.com/dgrapov/DeviumWeb.

581 [40] J. Ernst, Z. Bar-Joseph, STEM: a tool for the analysis of short time series gene expression data.
582 BMC bioinformatics 7(1) (2006) 191.

583 [41] J. Xia, N. Psychogios, N. Young, D.S. Wishart, MetaboAnalyst: a web server for metabolomic
584 data analysis and interpretation. Nucl. Acids Res. 37(suppl_2) (2009) W652-W660.

585 [42] Z. Yan, D. Wang, H. Cui, D. Zhang, Y. Sun, H. Jin, X. Li, X. Yang, H. Guo, X. He, Phytotoxicity
586 mechanisms of two coumarin allelochemicals from *Stellera chamaejasme* in lettuce seedlings, Acta
587 Physiol. Plant. 38 (2016) 248.

588 [43] R. Kumar, S. Mahey, R. Arora, J. Mahajan, V. Kumar, S. Arora, Insights into biological
589 properties of less explored bark of industrially important *Acacia catechu* Willd, Ind. Crops Prod. 138
590 (2019) 111486.

591 [44] R.C. Smart, E. Hodgson, Molecular and biochemical toxicology, John Wiley & Sons, 2018.

592 [45] B. Ganem, From glucose to aromatics: recent developments in natural products of the shikimic
593 acid pathway, Tetrahedron, 34 (1978) 3353-3383.

594 [46] O. Titiz, M. Tambasco-Studart, E. Warzych, K. Apel, N. Amrhein, C. Laloi, T.B. Fitzpatrick,
595 PDX1 is essential for vitamin B6 biosynthesis, development and stress tolerance in Arabidopsis, The
596 Plant J. 48 (2006) 933-946.

597 [47] M.F. Dunn, D. Niks, H. Ngo, T.R. Barends, I. Schlichting, Tryptophan synthase: the workings
598 of a channeling nanomachine, Trends Biochem. Sci. 33 (2008) 254-264.

599 [48] S. Raboni, S. Bettati, A. Mozzarelli, Tryptophan synthase: a mine for enzymologists, Cell.
600 Molecul. Life Sci. 66 (2009) 2391-2403.

601 [49] M. Tambasco-Studart, O. Titiz, T. Raschle, G. Forster, N. Amrhein, T.B. Fitzpatrick, Vitamin
602 B6 biosynthesis in higher plants. P. Natl. A. Sci. 102(38) (2005) 13687-13692

603 [50] P. Bilski, M.Y. Li, M. Ehrenshaft, M.E. Daub, C.F. Chignell, Vitamin B6 (pyridoxine) and its
604 derivatives are efficient singlet oxygen quenchers and potential fungal antioxidants. Photochem.
605 Photobiol. 71(2) (2000) 129-134

606 [51] F. Busch, C. Rajendran, O. Mayans, P. Löffler, R. Merkl, R. Sterner, TrpB2 enzymes are O-
607 phospho-L-serine dependent tryptophan synthases, Biochem. 53 (2014) 6078-6083.

608 [52] C.L. Ho, K. Saito, Molecular biology of the plastidic phosphorylated serine biosynthetic pathway
609 in *Arabidopsis thaliana*, Amino acids, 20 (2001) 243-259.

610 [53] C. Won, X. Shen, K. Mashiguchi, Z. Zheng, X. Dai, Y. Cheng, H. Kasahara, Y. Kamiya, J.
611 Chory, Y. Zhao, Conversion of tryptophan to indole-3-acetic acid by tryptophan aminotransferases
612 of Arabidopsis and YUCCAs in Arabidopsis, Proceedings of the National Academy of Sciences, 108
613 (2011) 18518-18523.

614 [54] L. Nebo, R.M. Varela, J.M. Molinillo, O.M. Sampaio, V.G. Severino, C.M. Cazal, M.F. das
615 Grac¸as Fernandes, J.B. Fernandes, Macías, F. A., Phytotoxicity of alkaloids, coumarins and
616 flavonoids isolated from 11 species belonging to the Rutaceae and Meliaceae families. Phytochem.
617 Lett. 8 (2014) 226-232.

618 [55] S. Jan, T. Parween, T. Siddiqi, Anti-oxidant modulation in response to gamma radiation induced
619 oxidative stress in developing seedlings of *Psoralea corylifolia* L, J. Environ. Radioact. 113 (2012)
620 142-149.

621 [56] D. Solecka, Role of phenylpropanoid compounds in plant responses to different stress factors.
622 Acta Physiol. Plantarum 19(3) (1997) 257-268.

623 [57] G. Hari, K. Vadlapudi, P.D. Vijendra, J. Rajashekar, T. Sannabommaji, G. Basappa, A
624 combination of elicitor and precursor enhances psoralen production in *Psoralea corylifolia* Linn.
625 suspension cultures. Ind. Crops Prod. 124 (2018) 685-691.

626 [58] H. Miyagawa, H. Toda, T. Tsurushima, T. Ueno, J. Shishiyama, Accumulation of tryptamine in
627 barley leaves irradiated with UV light, Biosci. Biotech. Biochem. 58 (1994) 1723-1724.

[59] T. Fujiwara, S. Maisonneuve, M. Isshiki, M. Mizutani, L. Chen, H.L. Wong, T. Kawasaki, K. Shimamoto, Sekiguchi lesion gene encodes a cytochrome P450 monooxygenase that catalyzes conversion of tryptamine to serotonin in rice, J. Biol. Chem. 285 (2010) 11308-11313.

[60] S. Park, T.N.N. Le, Y. Byeon, Y.S. Kim, K. Back, Transient induction of melatonin biosynthesis in rice (*Oryza sativa* L.) during the reproductive stage, J. Pineal Res. 55 (2013) 40-45.

[61] S. Kang, K. Kang, K. Lee, K. Back, Characterization of tryptamine 5-hydroxylase and serotonin synthesis in rice plants, Plant Cell Rep. 26 (2007) 2009-2015.

[62] H. Kaur, S. Mukherjee, F. Baluska, S.C. Bhatla, Regulatory roles of serotonin and melatonin in abiotic stress tolerance in plants, Plant Sign. Behav. 10 (2015) e1049788.

Table 1. One-way ANOVA results showing the effect of umbelliferone over the time-course study.

Metabolites	P-Values	Class
Maltose	1.83E-07	Sugar
Phosphorylcholine	4.02E-07	Sphingolipid
beta-Sitosterol	0.0001	Lipid
Xylulose	0.0001	Sugar
Ribose	0.0002	Sugar
Pyrocatechol	0.0002	Alcohol (catechol)
6-deoxyglucose	0.0015	Sugar
5-Dehydroquinic acid	0.0026	Alicyclic acid
Myricetin	0.0029	Flavonol
Trans-Aconitate	0.0044	Tricarboxylate
Digalacturonic acid	0.0068	Glycan
Spermine	0.0107	Amine
Palmitic acid	0.0112	Fatty acid
D-Panose	0.0197	Sugar
Tyrosine	0.0217	Amino acids
Isohexonic acid	0.0235	Carboxylic acid
Indoleacetic acid	0.0273	Carboxylic acid
Tryptamine	0.0299	Alkaloid
3-Nitro-L-Tyrosine	0.0313	Nitrated amino acid
3-Amino-2,3-dihydrobenzoic acid	0.0335	Carbocyclic acid
Trehalose	0.0359	Sugar
Hypotaurine	0.0467	Sulfinic acid

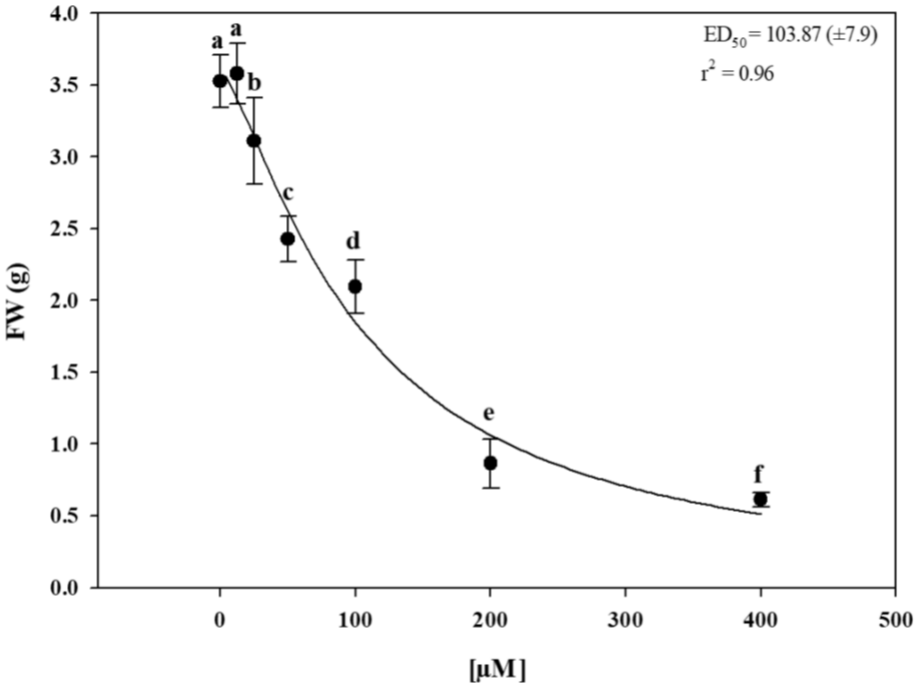

660

661 **Figure 1:** Dose-response curve evaluated on a FW base of *Triticum durum* cv. Opera seedlings treated
662 for 10 days with different doses (0, 12.5, 25, 50, 100, 200, 400 µM) of umbelliferone. Data were
663 analyzed through one-way ANOVA using LSD as post hoc ($P \leq 0.05$). ED_{50} (µM) value was
664 calculated through a log-logistic equation fitting the total FW data gotten from seedlings treated with
665 different doses of the allelochemical. The curve pointed out a significance level of $P < 0.001$. Bars
666 indicate standard deviation. n=5.

667

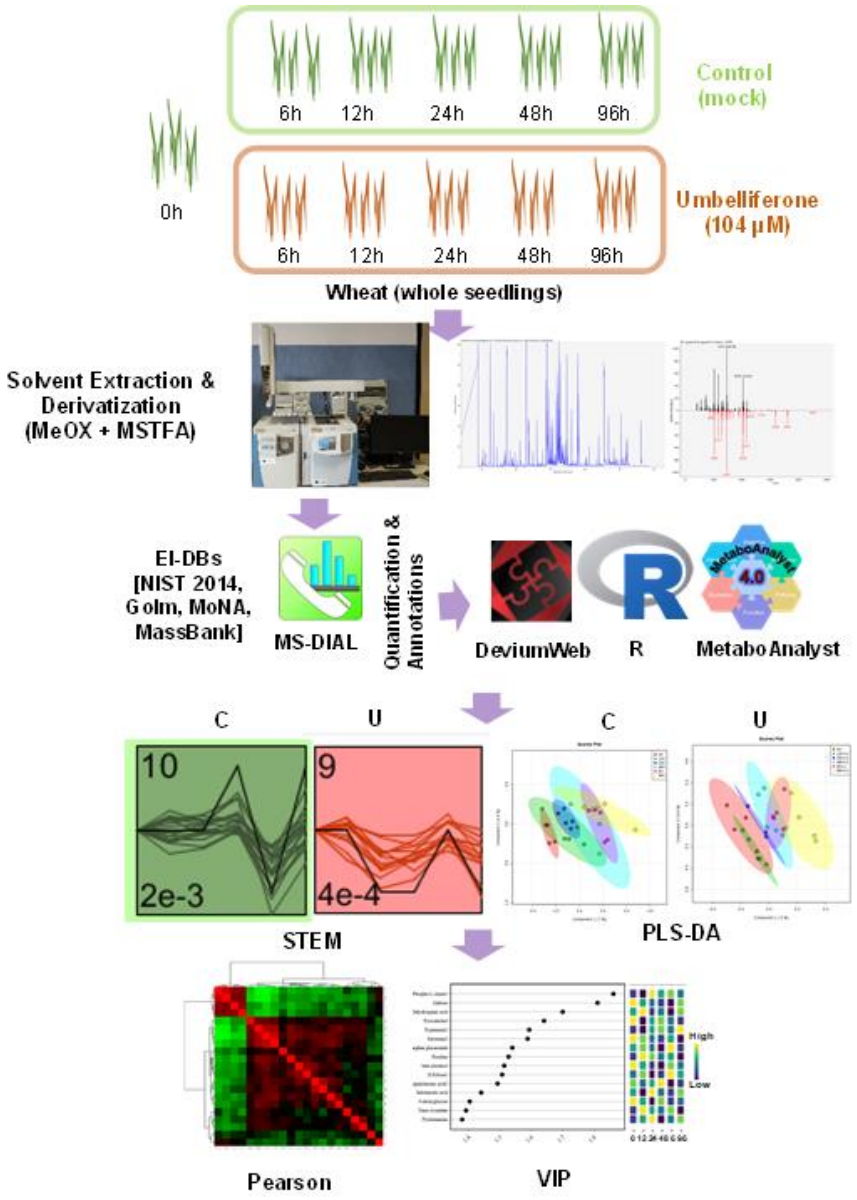

Figure 2. Schematic diagram displaying the experimental design, platform and software tools used for the analysis of metabolomic changes in wheat seedlings subjected to umbelliferone elicitation.

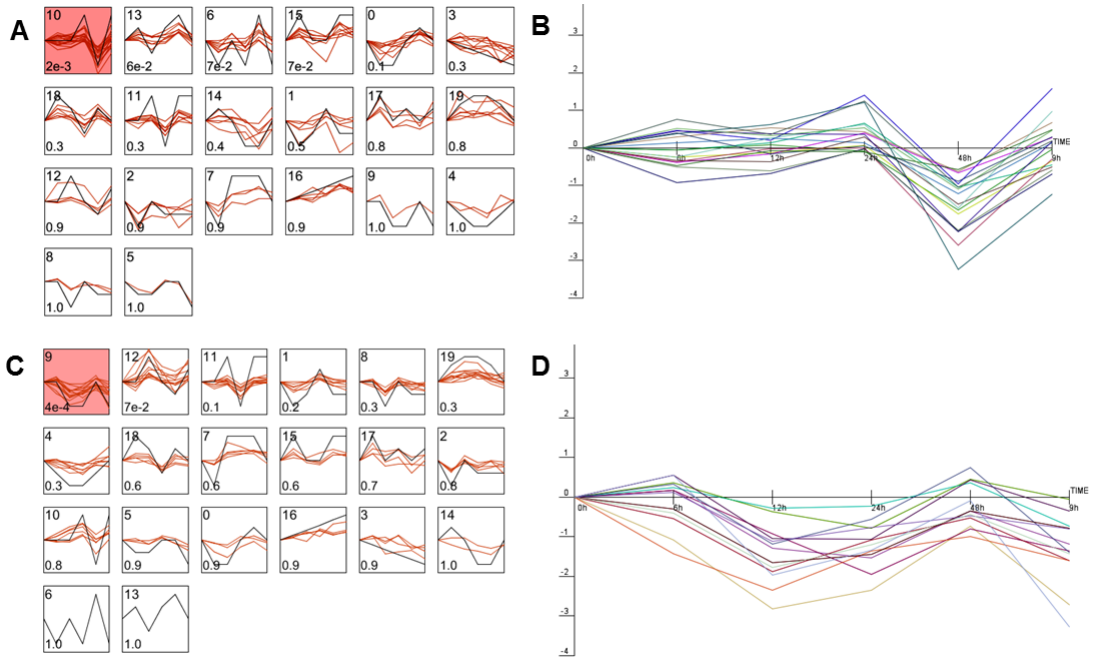

672

673 **Figure 3. Time course changes in the control and umbelliferone treated wheat seedlings.** (A)
674 Model profiles displaying the time-sensitive changes in metabolite abundance in control plants; (B)
675 Metabolite abundance profile in model # 10 (statistically significant) in control plants; (C) Model
676 profiles displaying the time-sensitive changes in metabolite abundance in umbelliferone-treated
677 plants; (D) Metabolite abundance profile in model # 9 (statistically significant) in umbelliferone-
678 treated plants. In panels A and C, the number in the upper left on each model profile designates the
679 model number (out of total 20 models generated), and the number in the bottom left on each model
680 profile is the statistical significance of the model. n=5.

681

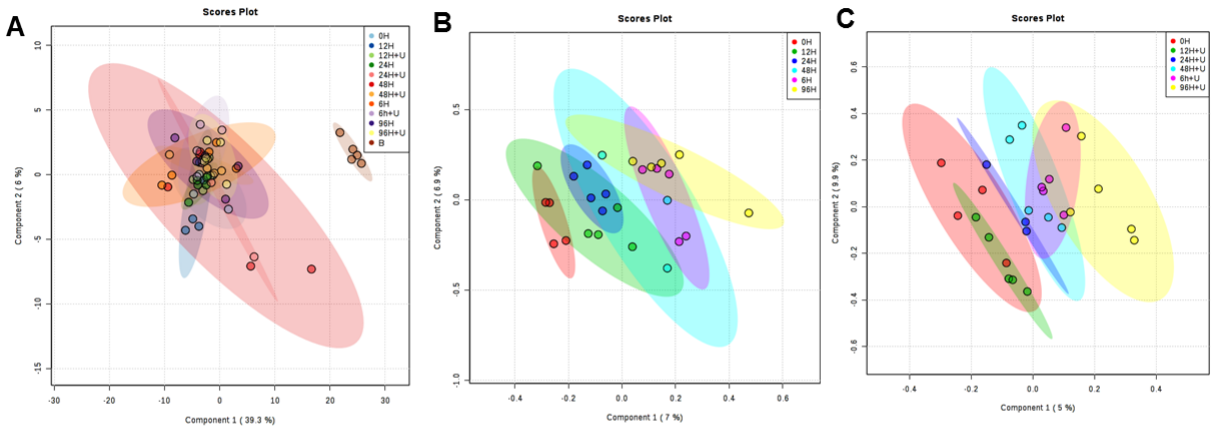

Figure 4. Multivariate (PLS-DA) analysis of the metabolomic changes. (A) PLS-DA displaying the separation of blank samples (B) from the rest of the samples showing system robustness; (B) PLS-DA showing clusters of various time points in control plants; (C) PLS-DA showing clusters of various time points in umbelliferone-treated plants. n=5.

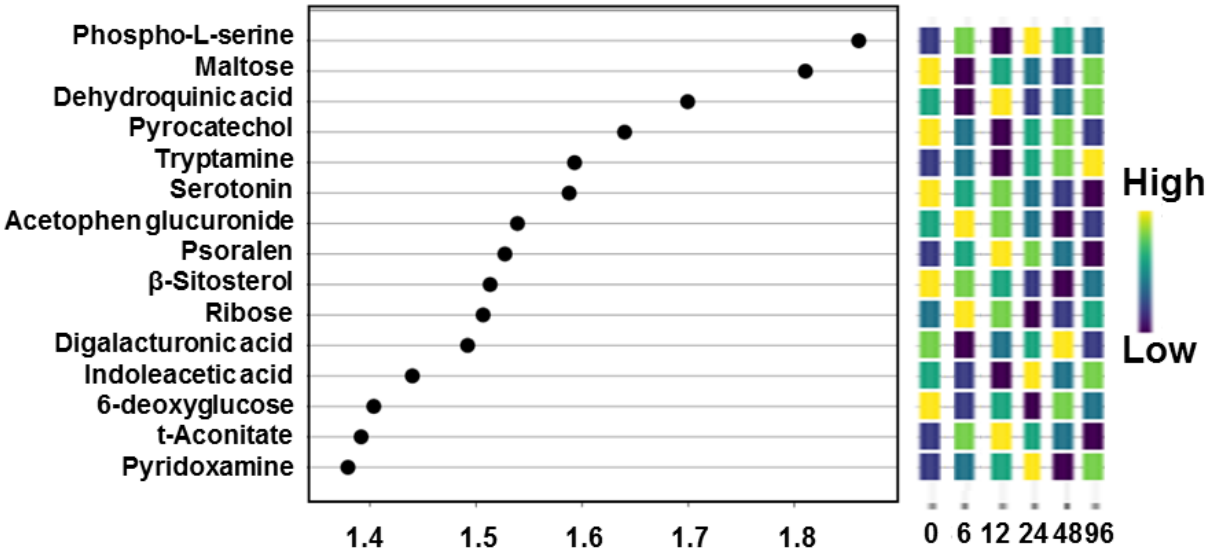

693

694 **Figure 5.** Top 15 metabolites (variables) based on VIP scores from PLS-DA analysis for each
695 umbelliferone treatment time points (0 h, 6 h, 12 h, 24 h, 48 h, 96 h). The x-axis shows the correlation
696 scores whereas the y-axis corresponds to the metabolites identified. Color bars show median intensity
697 of variable in the respective group. n=5.

698

699

700

701

702

703

704

705

706

707

708

709

710

711

712

Supplementary Materials

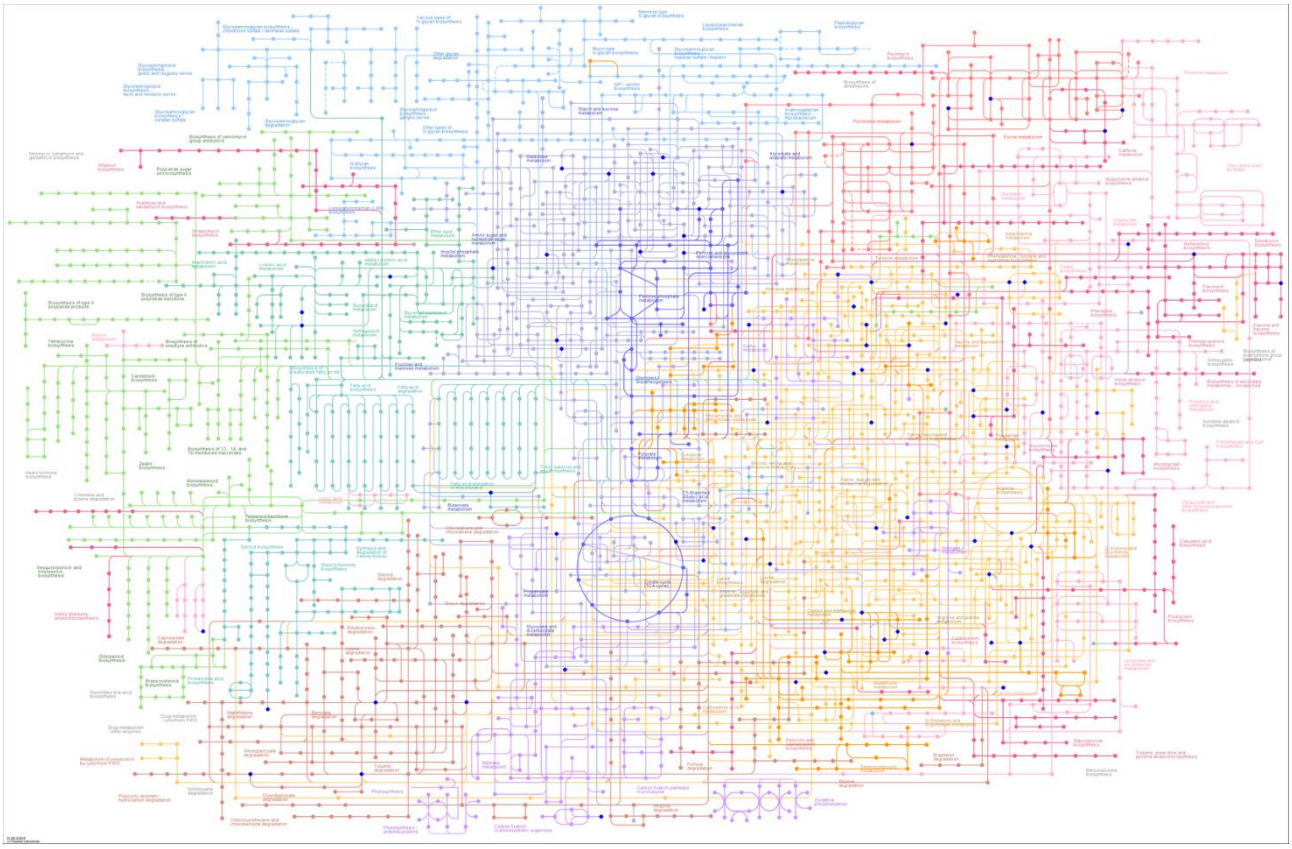

Supplementary Figure 1. Visual display of the coverage of metabolites quantified using our GC-MS platform for this metabolomics investigation. **(**KEGG-based metabolite mapped onto the KEGG metabolic pathway map (*blue dots* represent the mapped metabolites quantified in our study).

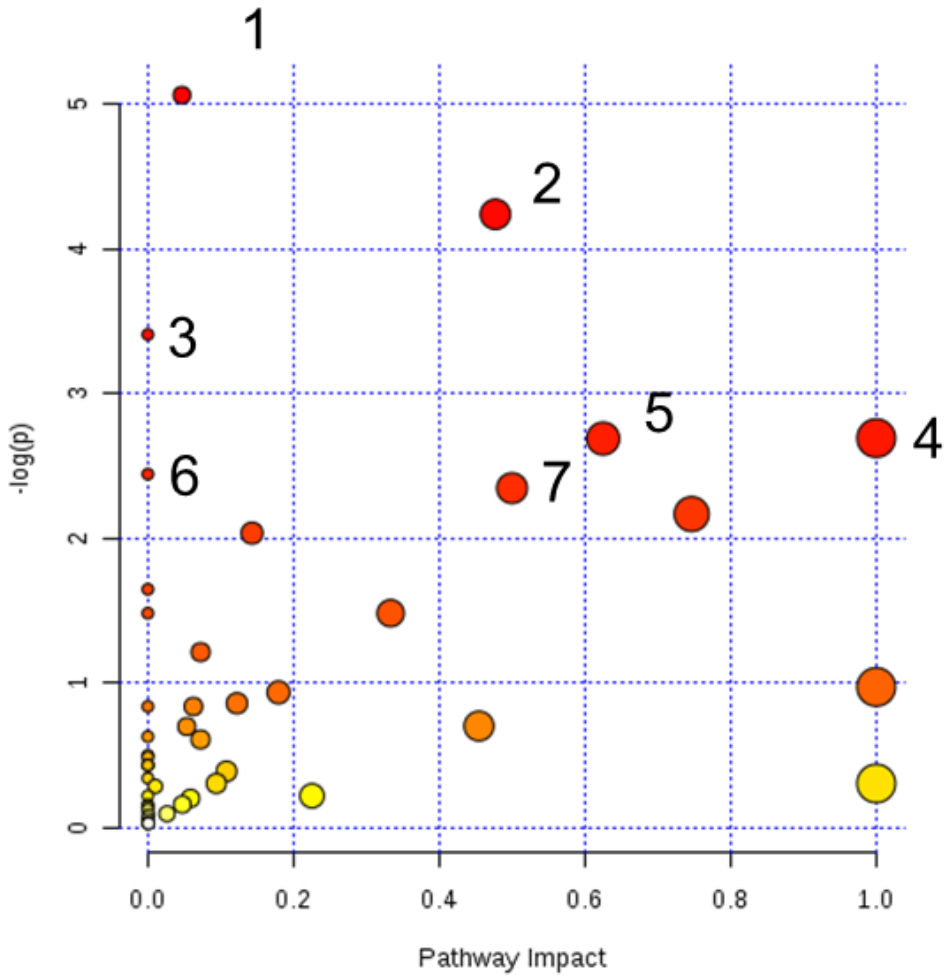

Supplementary Figure 2. KEGG-based pathway enrichment analysis displaying the wheat seedling metabolome as covered using our GC-MS platform. Pathway names: 1-Glutathione metabolism, 2-Arginine and proline metabolism, 3-Amino acyl-tRNA biosynthesis, 4-Taurine and hypotaurine metabolism, 5-Tryptophan metabolism, 6-beta-Alanine metabolism, and 7-Isoquinoline alkaloid biosynthesis.

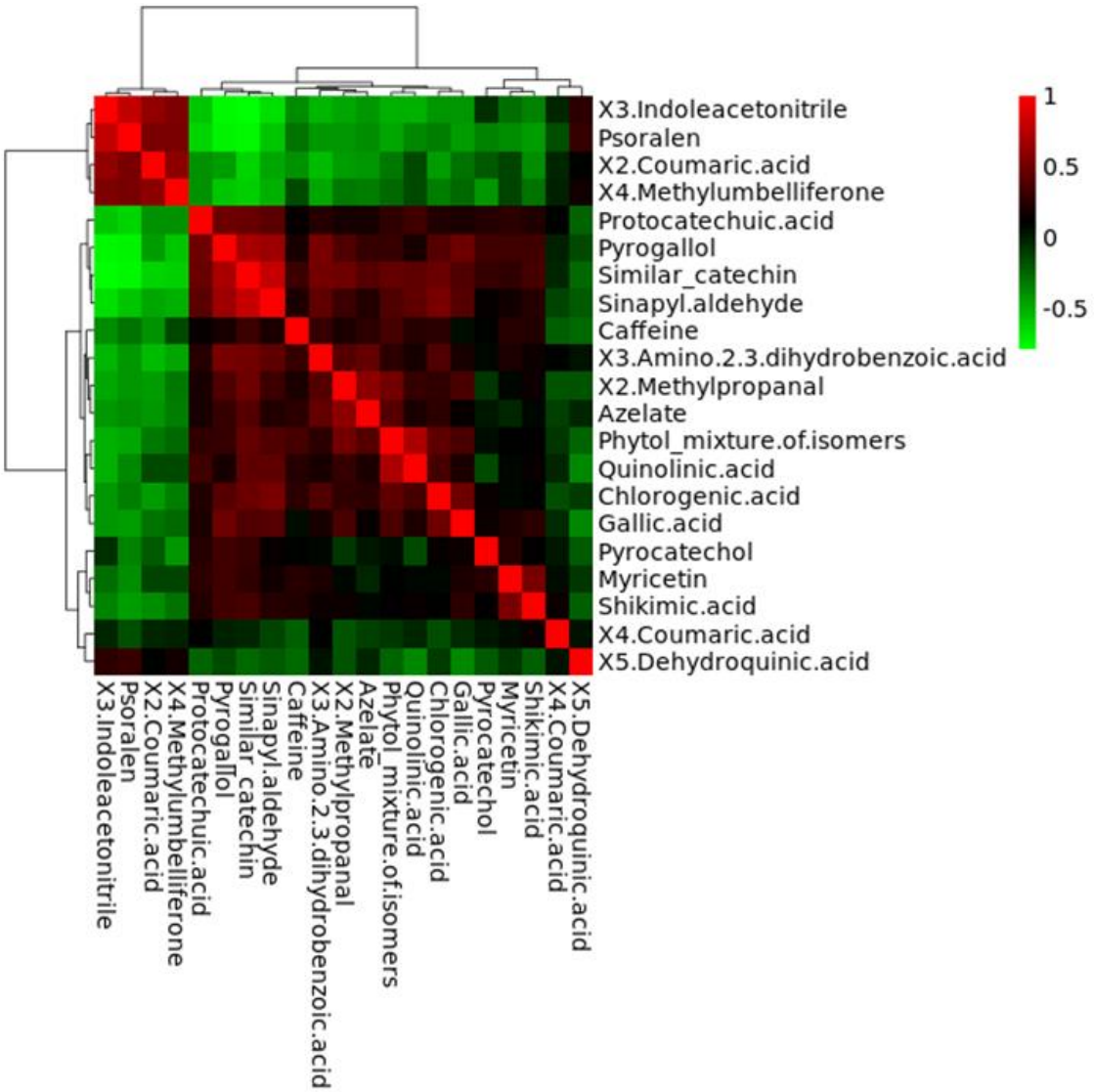

730

731 **Supplementary Figure 3.** High Pearson (metabolite-metabolite) correlation of umbelliferone-
732 derived metabolites and polyphenol metabolism-derived metabolites.

733

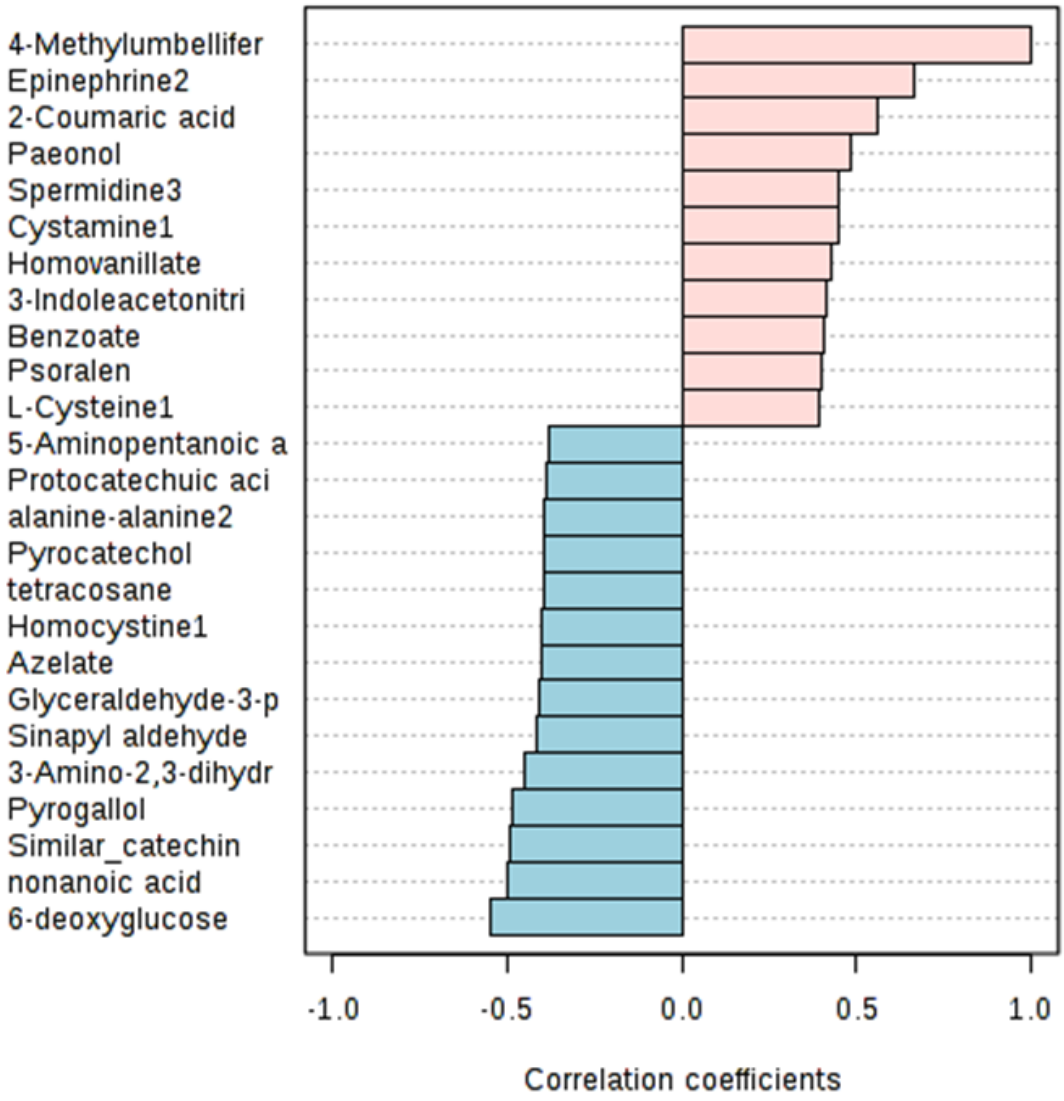

734

735 **Supplementary Figure 4.** High Pearson (metabolite-metabolite) correlation of umbelliferone-
736 derived metabolites with other quantified metabolites in the study.

737

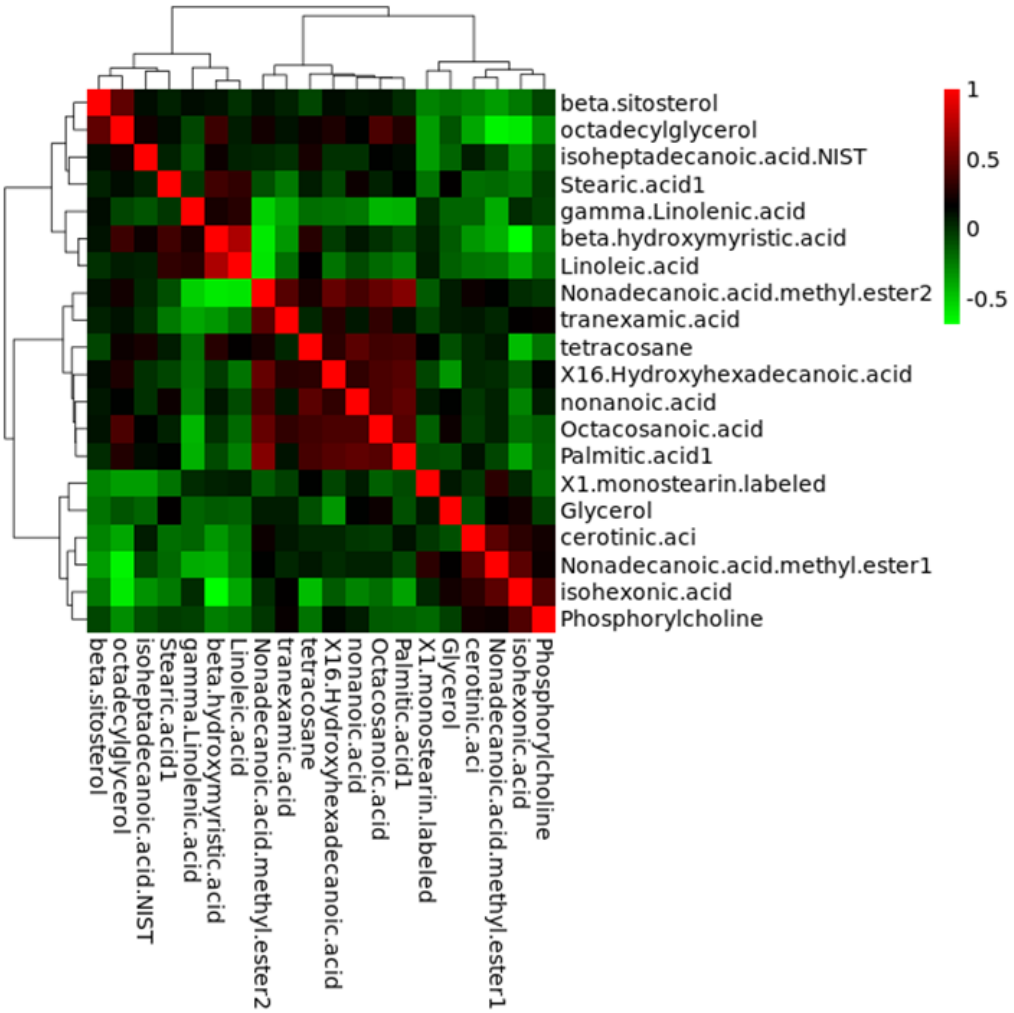

Supplementary Figure 5. High Pearson (metabolite-metabolite) correlation of fatty acids.

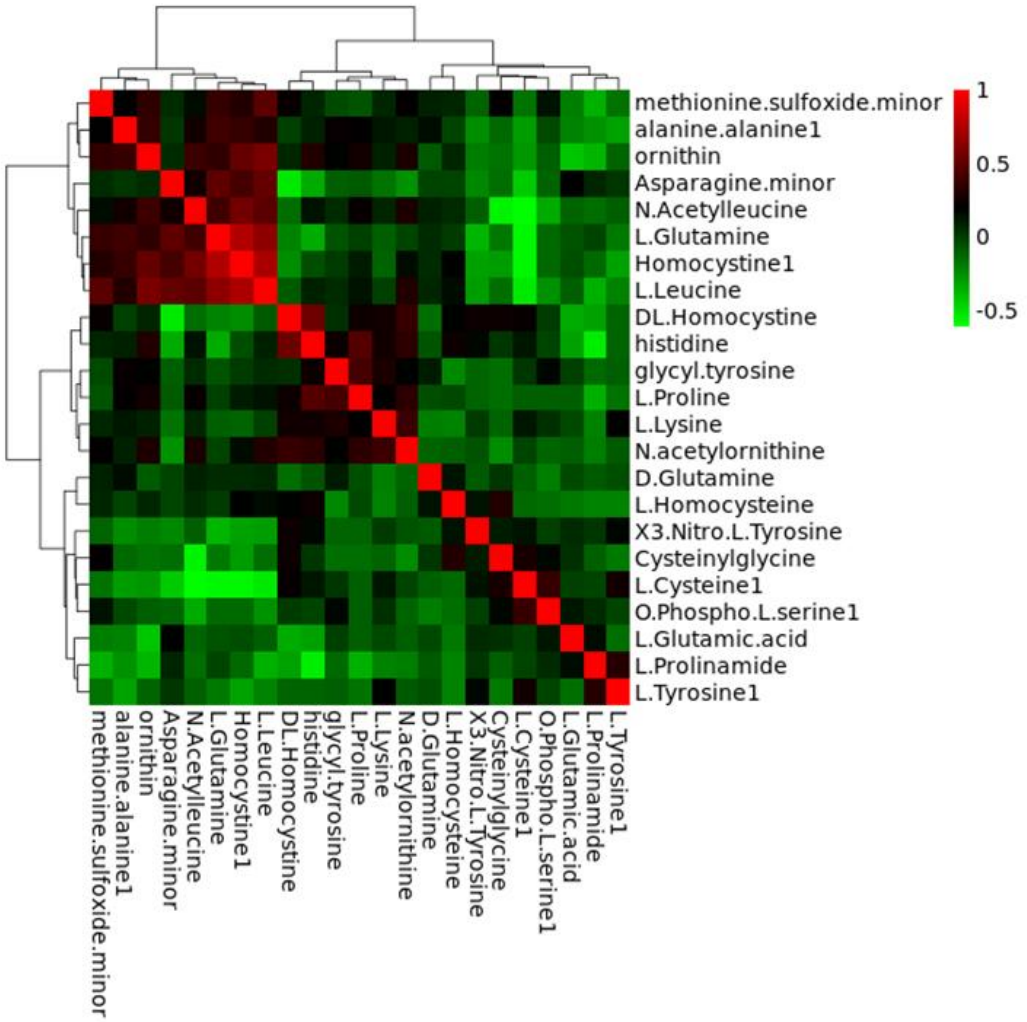

747

748 **Supplementary Figure 6.** High Pearson (metabolite-metabolite) correlation of amino acids.

749

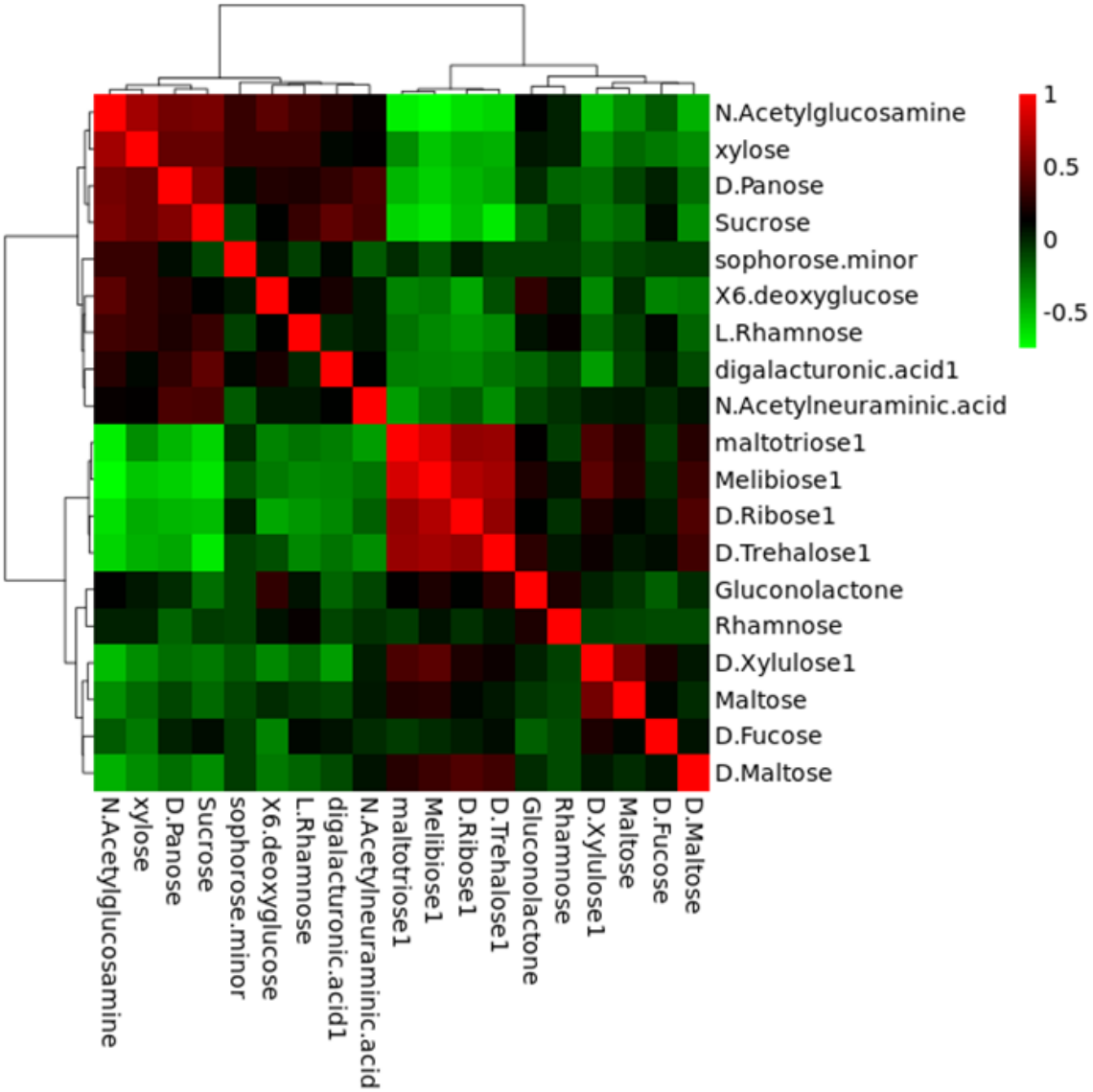

Supplementary Figure 7. High Pearson (metabolite-metabolite) correlation among carbohydrates.

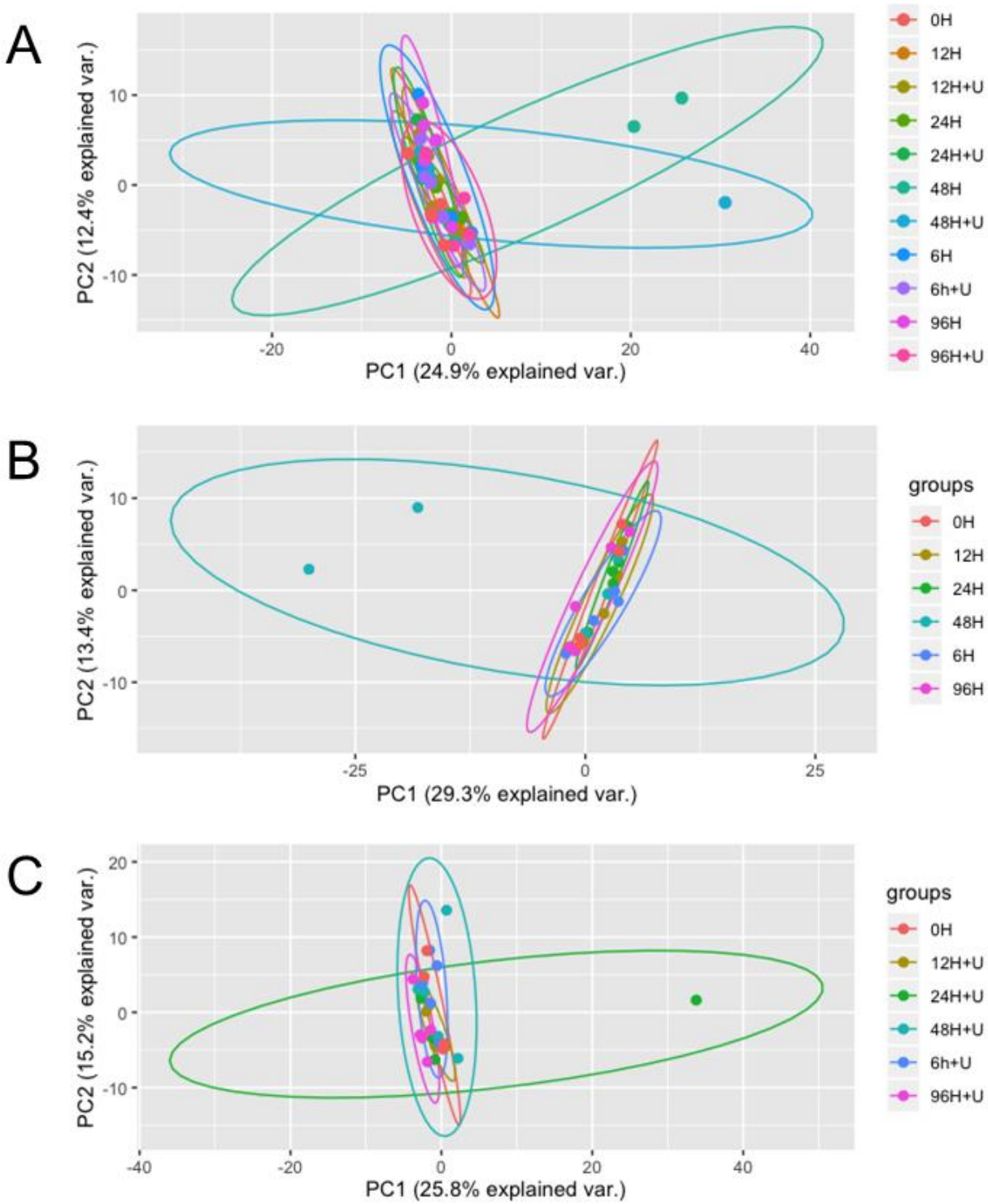

Supplementary Figure 8. Unsupervised principal component analysis (PCA) displaying the first 2 PCs for (A) all samples (control + Umbelliferone treatment) and time points together, (B) Control samples and time points, and (C) Umbelliferone treatment samples and time points.